NASA Technical Memorandum 104226

Fully Integrated Aerodynamic/Dynamic Optimization of Helicopter Rotor Blades

Joanne L. Walsh
William J. LaMarsh II
Howard M. Adelman

February 1992

National Aeronautics and
Space Administration

Langley Research Center
Hampton, Virginia 23665

FULLY INTEGRATED AERODYNAMIC/DYNAMIC OPTIMIZATION OF HELICOPTER ROTOR BLADES

by

Joanne L. Walsh*
NASA Langley Research Center
Hampton, Virginia

William J. LaMarsh II**
UNISYS Corporation
Hampton, Virginia

and

Howard M. Adelman†
NASA Langley Research Center
Hampton, Virginia

Abstract

This paper describes a fully integrated aerodynamic/dynamic optimization procedure for helicopter rotor blades. The procedure combines performance and dynamics analyses with a general purpose optimizer. The procedure minimizes a linear combination of power required (in hover, forward flight, and maneuver) and vibratory hub shear. The design variables include pretwist, taper initiation, taper ratio, root chord, blade stiffnesses, tuning masses, and tuning mass locations. Aerodynamic constraints consist of limits on power required in hover, forward flight and maneuver; airfoil section stall; drag divergence Mach number; minimum tip chord; and trim. Dynamic constraints are on frequencies, minimum autorotational inertia, and maximum blade weight. The procedure is demonstrated for two cases. In the first case the objective function involves power required (in hover, forward flight, and maneuver) and dynamics. The second case involves only hover power and dynamics. The designs from the integrated procedure are compared with designs from a sequential optimization approach in which the blade is first optimized for performance and then for dynamics. In both cases, the integrated approach is superior.

---

*Research Engineer, Interdisciplinary Research Office, Member AIAA, AHS

**Computer Programmer/Analyst

† Deputy Head, Interdisciplinary Research Office, Associate Fellow AIAA, Member AHS, ASME

Symbols

AI	autorotational inertia, $\sum_{j=1}^{ns} W_j r_j^2$ (lbm-in^2)
AI_{min}	minimum autorotational inertia (lbm-in^2)
c_d	airfoil section drag coefficient
$c_{d_{all}}$	maximum allowable section drag coefficient
$c_{d_{max}}^{\psi}$	largest section drag coefficient at azimuthal angle ψ
C_D	rotor coefficient of drag
C_L	rotor coefficient of lift
c_r	root chord (in)
c_t	tip chord (in)
$c_{t_{min}}$	minimum tip chord (in)
DV_i	ith design variable
DV_i^*	normalizing factor for ith design variable
EI_{xx}	chordwise bending stiffness (lb-ft^2)
EI_{zz}	flapwise bending stiffness (lb-ft^2)
f_i	ith frequency (per rev)
f_{il}	lower bound on ith frequency (per rev)
f_{iu}	upper bound on ith frequency (per rev)
F	objective function
g_i	ith constraint function
GJ	torsional stiffness (lb-ft^2)
ITER	number of trim iterations
$ITER_{max}$	maximum number of trim iterations allowed
k_i	ith weighting factor in objective function
m_i	ith tuning mass (lbm)

N	number of blades
n	integer
nP	frequency, integer multiple of rotor rotational frequency (per rev)
ns	number of structural segments
NDV	number of design variables
P_a	power available (hp)
P_h	power required in hover (hp)
$P_{h_{ref}}$	reference power required in hover (hp)
P_{ff}	power required in forward flight (hp)
$P_{ff_{ref}}$	reference power required in forward flight (hp)
P_m	power required in maneuver (hp)
$P_{m_{ref}}$	reference power required in maneuver (hp)
R	blade radius from center of rotation (in)
r	distance along blade from center of rotation (in)
r_j	distance from center of rotation to center of jth segment (in)
$S_{4_{ff}}$	4 per rev nonrotating vertical hub shear in forward flight (lbf)
$S_{4_{ref}}$	reference 4 per rev nonrotating vertical hub shear in forward flight (lbf)
$S_{N_{ff}}$	N per rev vertical nonrotating hub shear in forward flight (lbf)
$S_{N_{ref}}$	reference N per rev nonrotating vertical hub shear in forward flight (lbf)
t_i	ith torsional frequency (per rev)
W	total blade weight (lbm)
W_{max}	maximum blade weight (lbm)
W_j	total weight of jth structural segment (lbm)
y_i	location of ith tuning mass
y_{tr}	point of taper initiation
Δf	increment used in frequency window (per rev)
θ_{tw}	maximum pretwist (deg)
Ψ	azimuth angle, zero over tail (deg)

Introduction

The multidisciplinary nature of the helicopter rotor blade design process involves several disciplines including aerodynamics, dynamics, structures, and acoustics. Most rotor optimization has been applied to single disciplines. For example, rotor dynamic optimization is discussed in Refs. 1-6. Rotor structural optimization is discussed in Refs. 1 and 7. Rotor blades are designed for optimum performance in Refs. 1, 8 and 9. Recently, techniques and strategies for integrating disciplines in rotorcraft design procedures have been emerging. Such a plan is described in Refs. 10 and 11.

Progress has been made in developing integrated procedures for rotor blade design (Refs. 12-14). Reference 12 describes an optimization procedure which designs a rotor blade for combined aerodynamics, dynamics, and structures in stages. The blade is first designed for aerodynamic performance with power required in hover as the objective function, chord and twist as design variables, and a constraint on the autorotational inertia of the blade. The resulting optimum design results in a shift in the blade natural frequencies due to changes in the blade chord and twist distributions. A blade-frequency placement optimization is then performed to bring the blade natural frequencies to within prescribed windows. Finally, the rotor power is minimized with all the constraints (frequency, stress, fatigue life, and aeroelastic stability). References 13 and 14 describe the formulation of a multidisciplinary approach to rotor blade design for improved performance and reduced fuselage vibrations. The objective function is a linear combination of power required in hover, power required in forward flight, and vibratory load. The design variables are perturbations from the initial design of the following: linear and/or nonlinear twist and chord distributions, stiffnesses (flapwise, chordwise, and torsional), section mass and section moment of inertia. The constraints are a lower bound on blade weight for minimum autorotational inertia capability, an upper bound on section angle of attack at the blade tip, and a lower bound on tip chord. The rotor solidity and frequencies are constrained to be close to the initial values. The constraint on solidity is imposed so that the optimized design will have the same performance as the initial blade without compromising maneuvering capability. Reference 14 extended this work to included additional design variables - blade sweep and offsets of the center of gravity from the aerodynamic center.

In the present work, a fully integrated aerodynamic/dynamic optimization procedure is described. The procedure accounts for aerodynamic performance and dynamics simultaneously. In this work, constraints are enforced on power required, airfoil section stall, drag divergence Mach number, minimum tip chord, trim, rotor frequencies, autorotational inertia, and blade weight. This procedure accounts for the interactions between disciplines by simultaneously changing the design variables to satisfy the design requirements and optimizing a composite measure of both performance and dynamics. The procedure is similar to that of Refs. 13 and 14 but differs in several ways. First, in the present work, stiffness distributions, tuning masses, and tuning mass locations are design variables. Second, a maneuver flight condition is included in the objective function and constraints. Third, no constraint on solidity is necessary since the the blade is designed for a constant lift in forward flight and a constant lift in maneuver. Fourth, the frequency constraints are formulated so that the frequencies are away from integer multiples of the rotor speed and are not confined to be near the initial frequency values.

This paper describes the application of the optimization procedure to the design of a 1/6th scale model of a rotor blade for a utility helicopter. Results for two composite objective functions are presented - one involving performance (in hover, forward flight, and maneuver) and dynamics; the other involving performance in hover and dynamics. For both cases comparisons are made between ***integrated*** and ***sequential*** optimization approaches to rotor blade design. The integrated approach accounts for the interactions between disciplines by simultaneously changing

both aerodynamic and dynamic design variables and including both performance and dynamics in the objective function and constraints. The sequential approach is to optimize the blade first for performance using only aerodynamic design variables and performance constraints. This performance-optimized design is then optimized for dynamics by adjusting the blade stiffnesses and adding tuning masses. The paper demonstrates that the integrated optimization approach is generally better than the sequential approach from the standpoint of better designs.

Rotor Blade Design Considerations

In the present work the rotor blade is designed for performance and dynamics for three flight conditions: hover, forward flight, and maneuver. The maneuver flight condition simulates a sustained pull-up maneuver in terms of a load factor on the forward flight lift requirement. Satisfactory aerodynamic performance is defined by the following four requirements. First, the power required for any flight condition must be less than the available power. Second, airfoil section stall along the retreating side of the rotor disk must be avoided and the section drag divergence Mach number on the advancing side of the rotor disc must not be exceeded. The stall requirements are handled by requiring the airfoil sections distributed along the rotor blade operate at section drag coefficients less than a specified value, $c_{d_{all}}$. Third, the rotor must trim at each flight condition. Fourth, the blade tip chord must be larger than a prescribed minimum value, $c_{t_{min}}$.

For this work, satisfactory dynamics is defined in terms of limits on vibrational frequencies. The blade is designed so that the natural frequencies (both bending and torsional) are away from integer multiples of the rotor speed. The blade must have sufficient autorotational inertia in case of engine failure. In addition to satisfying these design requirements, the blade weight must not exceed some upper limit, W_{max}.

Optimization Formulation

Design Variables

The nineteen design variables shown in Fig. 1 consist of aerodynamic quantities describing the blade planform and dynamic quantities describing the blade structural properties. The four aerodynamic design variables are the point of taper initiation y_{tr}, root chord c_r, taper ratio c_r/c_t, and maximum pretwist θ_{tw}. The blade is rectangular to y_{tr} and then tapers linearly to the tip. The pretwist (blade structural and aerodynamic twist are assumed to be the same) varies linearly from the center of rotation to the tip. Nine dynamic design variables include the blade chordwise, flapwise, and torsional stiffnesses (denoted by EI_{xx}, EI_{zz}, and GJ, respectively) at the blade root, point of taper initiation, and blade tip. The stiffnesses are assumed to vary linearly between these three points. Although the three stiffnesses are treated as independent variables, they are in fact related at a given cross section by a single set of cross-sectional dimensions and material properties. However, in the present formulation this relationship is not incorporated. This reconciliation of stiffnesses and their physical realizability are assumed to be relegated to a separate design level where the cross section of the blade is determined. In principle, this multilevel decomposition of the rotor blade design is described in Ref. 11. A demonstration of the feasibility of this type of decomposition where independent global design variables are determined at one level and the reconciliation of the relationships among the global variables using detailed design variables is done at a lower level is described in Ref. 15. In the absence of the lower level the mutual dependence of the stiffnesses and physical realizability of the corresponding cross sections is accounted for by initialization to an existing blade and the expectation that these variables will not depart much from their initial values. The remaining six dynamic design variables are three tuning masses (denoted by m_1, m_2, m_3) and their locations (denoted by y_1, y_2, and y_3). The total blade mass consists of the structural mass (which is assumed constant) plus the sum of the tuning masses. It is assumed that the center of gravity and aerodynamic offsets are coincident with the blade elastic axis. The number of blades, rotor radius, rotational velocity, airfoils, and airfoil distribution are preselected and fixed. Upper and lower bounds on the design variables are summarized in Table 1.

Constraints

In this section of the paper, the rotor blade design requirements are expressed as mathematical constraints. By convention a constraint function denoted by g_i is satisfied if it is less than or equal to zero. The constraints are grouped into performance constraints and dynamic constraints. The performance constraints are imposed for all three flight conditions. The dynamic constraints are imposed only in forward flight and maneuver. Parameters used in the constraints are summarized in Table 1.

Performance Constraints - Recall the performance constraints are on power required, trim, stall, and blade tip chord. The requirement that the powers required in hover, forward flight, and maneuver be less than the power available translates into three constraints

$$g_i = P_r/P_a - 1 \le 0 \qquad \text{for each flight condition} \qquad (1)$$

where P_r and P_a are the power required and the power available, respectively.

The requirement that the airfoil sections not stall in forward flight and maneuver and that the drag divergence Mach number be avoided translates into constraints on the airfoil section drag coefficient, c_d. This leads to 24 constraints per flight condition since the c_d's are evaluated at every 15 degrees around the azimuth. At a given azimuthal angle Ψ the constraint is formulated as

$$g_i = c_{d_{max}}^{\Psi}/c_{d_{all}} - 1 \le 0 \quad \Psi=15,30,45,...,360 \quad (2)$$

where $c_{d_{all}}$ is the allowable drag coefficient and $c_{d_{max}}^{\Psi}$ is the largest drag coefficient along the blade radius outside the reverse flow region at the azimuthal angle Ψ.

In this work, an isolated rotor analysis is used which trims the rotor to constant lift C_L and drag C_D and zero flapping angle relative to the shaft using collective, lateral cyclic and longitudinal cyclic pitch. Trimming to a constant lift ensures that the rotor has no loss in lift capability even if solidity decreases. The trim requirement is difficult to translate into a mathematical constraint. The trim constraint in forward flight and maneuver is implemented using the method developed in Ref. 8 which expresses the constraint in terms of the number of trim iterations ITER, the maximum number of trim iterations allowed $ITER_{max}$, and the design variables DV_i. The heuristic trim constraint is given by

$$g_i = (ITER\text{-}ITER_{max}+1)\left(\sum_{p=1}^{NDV} \frac{DV_p}{DV_p^*}\right) \le 0 \quad (3)$$

where NDV is the number of design variables, DV_p is the pth design variable and DV_p^* is a normalizing factor so that the each term in the summation is approximately equal to one and positive. In development of Eqn. 3 in Ref. 8, it was found that the addition of the summation term helped to improve convergence by imparting additional information to use in the search direction for new design variable values.

The final performance requirement is a constraint used to ensure that the blade tip chord does not become too small

$$g_i = 1 - c_t/c_{t_{min}} \le 0 \quad (4)$$

where c_t is the tip chord and $c_{t_{min}}$ is the minimum tip chord allowed. These four design requirements were used in the performance optimization procedure of Refs. 8 and 9 and are considered the performance constraints.

Dynamic Constraints - Recall the dynamic constraints are on frequencies, total blade weight, and autorotational inertia. The constraint on the kth frequency f_k (either a bending or a torsional frequency) is formulated such that the frequency is away from integer multiples of the rotor speed by an amount Δf

$$g_i = \frac{f_k}{f_{ku}} - 1 \le 0 \quad (5)$$

and

$$g_i = 1 - \frac{f_k}{f_{kl}} \le 0 \quad (6)$$

where f_{ku} has a value that is Δf below n+1 per rev and f_{kl} has a value that is Δf above n per rev for the applicable n. For example, suppose Δf is 0.1 per rev and f_4 is 5.6 per rev, then nP would be 5 per rev and (n+1)P would be 6 per rev. Thus f_{4u} and f_{4l} would be 5.9 per rev and 5.1 per rev, respectively. Formulating the constraints in this manner allow the frequencies to change provided they avoid approaching integer multiples of the rotor speed. This formulation is different from the approaches used in Refs. 12-14 where the frequencies are kept within prescribed windows close to the reference blade frequencies. In this work constraints are placed on frequencies in both forward flight and maneuver. Although these are the natural frequencies and should be independent of flight condition, the blade collective pitch may be different in forward flight and maneuver. Thus the amount of modal coupling would vary and it is possible that the frequencies could be different for the two flight conditions.

The constraint that the blade weight be less than some maximum value is formulated as follows

$$g_i = W/W_{max} - 1 \le 0 \quad (7)$$

where W is the total blade weight and W_{max} is the maximum allowable weight. The total blade mass is determined from the structural mass distribution (which is assumed constant) plus the sum of the tuning masses.

Finally, the blade must have enough autorotational inertia AI for safe autorotation in case of engine failure. The constraint is formulated so that the autorotational inertia of the blade is greater than some minimum value AI_{min}

$$g_i = 1 - AI/AI_{min} \le 0 \quad (8)$$

Objective function - The objective function used in this work is similar to the objective function defined in Refs. 10 and 11 which was a linear combination of power required (in hover, climb, forward flight, and maneuver) and hub shear. In the present work the climb term has been omitted. The objective function to be minimized is a combination of performance (the power required for each flight condition) and dynamics measure (the N per rev nonrotating vertical hub shear in forward flight where N is the number of blades) and is formulated as follows

$$F = k_1 \frac{P_h}{P_{h_{ref}}} + k_2 \frac{P_{ff}}{P_{ff_{ref}}} + k_3 \frac{P_m}{P_{m_{ref}}} + k_4 \frac{S_{N_{ff}}}{S_{N_{ref}}} \quad (9)$$

where P_h, P_{ff}, and P_m are the powers required in hover, forward flight, and maneuver, respectively. $S_{N_{ff}}$ is the N

per rev nonrotating vertical hub shear in forward flight. The terms k_1, k_2, k_3, and k_4 are weighting factors. $P_{h_{ref}}$, $P_{ff_{ref}}$, $P_{m_{ref}}$, and $S_{N_{ref}}$ are reference values used to normalize and nondimensionalize the objective function components.

Rotor Analyses

The analyses used in this work are the Langley-developed hover analysis program HOVT (a strip theory momentum analysis based on Ref. 16) and the comprehensive helicopter analysis program CAMRAD/JA (Ref. 17) for forward flight and maneuver. HOVT is used to predict power required in hover using nonuniform inflow (no wake is included). CAMRAD/JA is used to calculate rotor performance, loads, and frequencies. In this work the CAMRAD/JA analyses are performed with uniform inflow with empirical inflow correction factors. Both HOVT and CAMRAD/JA use tables of experimental two-dimensional airfoil data.

Optimization Methods

The optimization methods used in this work are the general purpose optimization program CONMIN (Ref. 18) and an approximate analysis used to reduce the number of HOVT and CAMRAD/JA analyses during the iteration process. CONMIN is a general purpose optimization program which uses the method of feasible directions for constrained function minimization. The approximate analysis is used to extrapolate the objective function and constraints with linear Taylor Series expansions using derivatives of the objective function and constraints with respect to the design variables. The assumption of linearity is valid over a suitably small change in the design variable values and will not introduce a large error into the analysis provided the changes are small. Errors which may be introduced by use of the approximate analysis are controlled by imposing "move limits" on each design variable during the iteration process. A move limit which is specified as a fractional change of each design variable value is imposed as an upper and lower design variable bound.

Implementation of Optimization Procedure

The optimization procedure (Fig. 2) consists of an outer loop denoted by "Cycle" and an inner loop denoted by "Iteration". First, preassigned parameters such as the blade radius, airfoil distribution, and number of blades are set. An optimization cycle is initiated. The aerodynamic and structural properties such as twist and chord distributions, radial station locations, solidity, blade weight, and autorotational inertia are calculated using the current design variable values in the box labelled "Design variable preprocessors". The HOVT analysis is then performed to obtain the power required in hover. Two CAMRAD/JA analyses (forward flight and maneuver) are then performed to obtain the power required, trim information, c_d's for the stall constraints, natural frequencies, and hub shears. This information is then used to formulate the objective function and constraints. Since CONMIN and the approximate analysis need derivatives of the objective function and constraints, a sensitivity analysis is performed to obtain finite difference derivatives of the objective function and constraints with respect to the design variables. These derivatives are obtained by perturbing each design variable one at a time and going through the design variable preprocessor, HOVT, and CAMRAD/JA analyses. The inner loop consists of CONMIN and the approximate analysis. New values for the design variables are obtained and the outer loop is re-entered. Convergence is obtained if the objective functions from three consecutive cycles are the same within a tolerance of 0.5×10^{-5}.

Test Problem

Shown in Fig. 3 is a 1/6th-scale wind tunnel model of a rotor blade for a four-bladed utility helicopter. This blade has a rectangular planform to 0.80R (80 percent radius) and then tapers to the tip with a 3-to-1 taper ratio. The blade has a radius of 56.22 in and a root chord of 5.40 in. Three sets of advanced airfoils are used along the blade. The RC(4)-10 airfoil (Ref. 19) is used to 82.5 percent radius, the RC(3)-10 (Ref. 20) airfoil is used from 87.5 to 92.5 percent radius, and the RC(3)-08 (Ref. 20) airfoil is used from 97.5 percent radius to the tip. Details of the blade can be found in Ref. 21. This blade will be referred to as the ***reference blade***.

An analytical model of the reference blade with 19 aerodynamic segments for HOVT, 50 structural segments and 18 aerodynamic segments for CAMRAD/JA is used to obtain values for the maximum allowable blade weight, the minimum value for the autorotational inertia, and the structural mass distribution. The flight conditions are a constant lift of 1-g (331 pounds, C_L=0.0081), propulsive force of 32 pounds (C_D=-0.000811), and an advance ratio of 0.35 for the forward flight condition and a constant lift of 401 pounds (C_L=0.00985), a propulsive force of 23 pounds (C_D=-0.000596), and an advance ratio of 0.3 for the maneuver flight condition. The maneuver flight condition is for a load factor of 1.22. From the modal analyses in CAMRAD/JA using ten bending modes and five torsional modes, it is found that only the first six bending frequencies are below 10 per rev and need to be constrained for a four-bladed rotor. Since f_1 corresponds to a rigid body mode and f_2 is the 1 per rev, the first two frequencies are not constrained. Constraints are placed on the first four bending frequencies (f_3, f_4 and f_6 flapping-dominated and f_5 lead-lag dominated) and the first two torsional frequencies (t_1 representing the rigid body torsional mode due to the control system stiffness and t_2 representing the first elastic torsional mode). From the procedure, this blade has a total weight of 3.05 lbs and an autorotational inertia value of 3411 lbm-in^2. In this work, the blade is to be designed so that the weight is not increased by more than 15 percent (W_{max}=3.5 lbs) and the autorotational inertia is increased by at least 1

percent (AI_{min}=3456 lbm-in^2) from that of the reference blade. The values for minimum tip chord ($c_{t_{min}}$), power available (P_a), and maximum allowable drag coefficient ($c_{d_{all}}$) are 1 in, 20 hp, and 0.1, respectively. A Δf of 0.1 per rev is used for the frequency constraints. Since a four-bladed rotor is used as the test problem, the 4 per rev nonrotating hub shear is used for S_N in the objective function given by Eqn 9. Parameters and flight conditions are summarized in Table 1.

The initial blade design (the starting point for the optimization) used in this work is shown in Fig. 4. This blade has a rectangular planform with a maximum pretwist of -9.0 deg and blade root chord of 5.40 in. This blade has the same root chord, mass distribution, and stiffness distributions at the root, 0.8R (point of taper initiation of the reference blade), and tip as the reference blade. The stiffnesses are assumed to vary linearly between these points. The nonstructural mass distribution only depends on the tuning masses and their locations. Note that the initial blade does not satisfy the minimum autorotational inertia requirement.

Results

The optimization procedure described previously is applied to two versions of the objective function given in Eqn. 9. For each case the normalizing factors $P_{h_{ref}}$, $P_{ff_{ref}}$, and $P_{m_{ref}}$ are each chosen to be 15 hp and $S_{N_{ref}}$ is chosen to be 2 lbf (based on analysis of the initial blade). The first case has an objective function which is a linear combination of the power required in hover, forward flight, and maneuver and the 4 per rev nonrotating vertical hub shear in forward flight. The reference blade was originally designed for performance. Therefore, the objective function is chosen to be one dominated by performance with little emphasis on dynamics. Of the three powers it is assumed that it is most important to reduce the power required in hover - it will have twice the weight as the other two powers. Several values were tried for the weighting factor on the hub shear term. It was found that to obtain the proper balance between performance and dynamics, k_4 has to be between one and two orders of magnitude less than k_1. Thus, for this case, the weighting factors are chosen to be k_1 =15.0, k_2=k_3=7.5, and k_4 = 0.025. This objective function will be referred to as Case 1. The second case has an objective function which is a linear combination of the power required in hover and the hub shear in forward flight (k_1=15.0, k_4=2.0, k_2=k_3=0.0). There are two reasons for investigating the second case. First, including only hover power in the objective function is similar to the conventional performance optimization described in Refs. 8 and 9. Second, it is of interest to see the effect of a larger emphasis on hub shear in the objective function. This objective function will be referred to as Case 2.

Integrated Optimization Results

A total of 19 design variables and 80 constraints are used. There are 4 aerodynamic design variables (y_{tr}, c_r, c_r/c_t, and θ_{tw}) and 15 dynamic design variables (EI_{xx} EI_{zz}, and GJ at the root, point of taper initiation, and tip; m_1; m_2; m_3; y_1, y_2, and y_3). The 54 performance constraints are: 3 constraints on power required (one per flight condition), 2 constraints on trim (one for forward flight and one for maneuver), 48 constraints on c_d (24 for forward flight and 24 for maneuver), and one constraint on minimum tip chord. The 26 dynamic constraints are: 24 frequency constraints (12 for forward flight and 12 for maneuver), a constraint on total blade weight, and a constraint on minimum autorotational inertia.

Case 1 Objective Function - The objective function is a combination of the power required (in hover, forward flight, and maneuver) and the 4 per rev nonrotating vertical hub shear in forward flight

$$F=15\frac{P_h}{P_{h_{ref}}}+7.5\frac{P_{ff}}{P_{ff_{ref}}}+7.5\frac{P_m}{P_{m_{ref}}}+0.025\frac{S_{4_{ff}}}{S_{4_{ref}}} \quad (10)$$

where $P_{h_{ref}}$, $P_{ff_{ref}}$, and $P_{m_{ref}}$ are each 15 hp, and $S_{4_{ref}}$ is 2 lbf. Results for the initial and integrated-optimized blades are summarized in Table 2. The optimized design has more pretwist (-16 degrees) and less root chord (4.38 in) than the initial design. The planform has changed from rectangular to tapered at 0.68R with a taper ratio of 1.79. The tuning masses are located about 0.395R to 0.475R with the two largest masses concentrated near 0.40R. The autorotational inertia increased 4.4 percent over the initial design (representing a 3 percent increase over the minimum requirement). There is a 9.5 percent increase in blade weight (part of the increase is due to the autorotational inertia requirement). All frequencies are away from per rev values. The powers required in hover, forward flight, and maneuver are reduced by 6.5, 6.7 and 4.1 percent, respectively, from the initial design. The forward flight hub shear is reduced from 2.19 to 1.89 lbf (representing a 13.7 percent reduction). This is a large reduction in spite of the small emphasis on hub shear in the objective function. The maneuver hub shear is reduced slightly from 0.95 to 0.92. Recall there is no constraint on maneuver hub shear and only forward flight hub shear is in the objective function.

The stiffness distributions for the initial and final designs are shown in Fig. 5. As shown in Fig. 5a, inboard of 0.5R the chordwise bending stiffness EI_{xx} is much higher than the initial design. From this point to about 0.9R, the stiffness is smaller than the initial design with the smallest value around 0.68R (the point of taper initiation). When point of taper initiation moved the stiffness distribution changed with it. Outboard of 0.9R the stiffness is slightly higher than the initial design. Inboard of 0.5R the flapwise bending stiffness EI_{zz} distribution is higher and outboard of

this location it is less than the initial design (see Fig. 5b). The torsional stiffness GJ is higher than the initial design inboard of 0.71R. GJ is smaller until 0.95R when it is slightly higher than the initial design (see Fig. 5c).

Comparison with Reference Blade - It is of interest to see how this integrated design compares with the reference blade for these same flight conditions. As shown in Table 3, the analysis predictions for the integrated design and the reference blade are similar. The integrated design has the same pretwist as the reference blade. Both planforms are similar with the integrated design having less solidity than the reference blade. The difference in planforms is primarily due to the choice of flight conditions. The reference blade was designed by nonoptimization techniques for slightly different flight conditions and design requirements.

Case 2 Objective Function - In Case 2, only hover performance and forward flight dynamics are included in the objective function

$$F = 15.0 \frac{P_h}{P_{h_{ref}}} + 2.0 \frac{S_{4_{ff}}}{S_{4_{ref}}} \qquad (11)$$

where $P_{h_{ref}}$ is 15 hp, and $S_{4_{ref}}$ is 2 lbf. Results are presented in Table 4 for the initial and the optimized designs. The optimized design has less pretwist (-8.1 degrees) and a smaller root chord (4.5 in) than the initial design. The planform has changed from a rectangular blade to one that tapers at 0.8R with a taper ratio of 1.36. The tuning masses are located between 0.25R and 0.41R with the largest mass at 0.29R and a slightly smaller mass at 0.25R. There is a 10 percent increase in blade weight. There is improvement in the power required for all flight conditions although not as much as in Case 1. The Case 2 design reduces the power required in hover and in forward flight by 3.9 and 4.4 percent, respectively. The two torsional frequencies (t_1 and t_2) are at their lower and upper bounds, respectively. The forward flight hub shear is reduced by 67.6 percent relative to the initial design (from 2.19 to 0.71 lbf). The maneuver hub shear is increased by 65.3 percent (recall there is no requirement on maneuver hub shear either in the objective function or constraints). The larger contribution of the hub shear term in the objective function seems to have a large influence on the resulting design. In this case, there is little change in the twist and less taper compared to Case 1.

The stiffness distributions are shown in Fig. 6. As shown in Fig. 6a, the chordwise stiffness EI_{xx} is slightly higher than the initial design inboard of the point of taper initiation and then decreases to a smaller value at the tip. The flapwise stiffness EI_{zz} is larger than the initial stiffness over the blade span (see Fig. 6b). The torsional stiffness GJ is also larger over the entire span with the greatest difference at the point of taper initiation (see Fig. 6c).

Integrated versus Sequential Optimization Results

It is of interest to compare the integrated optimization approach and a sequential optimization approach. The two approaches are summarized in Table 5 using the objective functions defined in Eqns. 10-15. The integrated approach is a one-step optimization procedure and uses all the aerodynamic and dynamic design variables, all the aerodynamic and dynamic constraints, and has an objective function which is a composite measure of performance and dynamics. The sequential approach is a two step optimization procedure. The first step consists of a performance optimization similar to that of Refs. 8 and 9. The blade is designed using only the four aerodynamic design variables (θ_{tw}, y_{tr}, c_r/c_t, c_r) and the performance constraints (power required, trim, stall, and minimum tip chord). In Step 2, the optimized-aerodynamic design variables are then held constant and the design is optimized for dynamics using the only the dynamic design variables (stiffnesses, tuning masses, and tuning mass locations) and dynamic constraints (frequencies, blade weight, and autorotational inertia) The trim constraint is still present . A sequential optimization procedure is done for both Case 1 and Case 2. Results are compared with those obtained using the integrated design approach.

Case 1 Objective Function - In the sequential optimization approach, the blade is optimized first for performance using only the aerodynamic design variables and constraints. In Step 1 the objective function in Eqn. 10 becomes

$$F = 15.0 \frac{P_h}{P_{h_{ref}}} + 7.5 \frac{P_{ff}}{P_{ff_{ref}}} + 7.5 \frac{P_m}{P_{m_{ref}}} \qquad (12)$$

where $P_{h_{ref}}$, $P_{ff_{ref}}$, and $P_{m_{ref}}$ are each 15 hp. The resulting blade is shown in the column labelled "Performance" in Table 6. The performance-optimized blade has a maximum pretwist of -16.0 degrees, is rectangular out to 0.51R, it has a taper ratio of 1.65, and a root chord of 4.73 in. This design requires 14.4 hp, 12.7 hp, and 11.8 hp in hover, forward flight, and maneuver, respectively.

Now, this performance-optimized blade is examined from the dynamics point-of-view by looking at the blade frequencies, hub shear, autorotational inertia, and blade weight. The blade frequencies have shifted from their original values. The second bending frequency f_4 (5.04 per rev) is unacceptable (recall frequency windows of 0.1 per rev were used, so this frequency should be between 5.1 and 5.9 per rev). Also the performance-optimized design has 4 per rev hub shears which increased by 32.4 percent (from 2.19 to 2.90 lbf) and 52.6 percent (from 0.950 to 1.45 lbf) over the initial values for forward flight and maneuver, respectively. The blade does not meet the minimum autorotational inertia requirement (recall the initial blade does not meet the minimum autorotational inertia requirement).

In Step 2, the performance-optimized design is optimized for dynamics by minimizing the 4 per rev hub shear in forward flight using dynamic design variables and dynamic constraints with performance design variables held constant. The objective function from Eqn. 10 is

$$F = \frac{S_{4_{ff}}}{S_{4_{ref}}} \tag{13}$$

where $S_{4_{ref}}$ is 2 lbf. Results for the dynamic optimization are shown in the column labelled "Dynamics" in Table 6. This is the final sequential optimum design. The unacceptable frequency f_4 is brought into the acceptable frequency window (5.10 per rev) with a slight shift in the other bending frequencies. This sequential optimum design has larger 4 per rev hub shears than the initial design (by 14.2 percent - from 2.19 to 2.50 lbf for forward flight - and by 38.9 percent - from 0.95 to 1.32 lbf for maneuver).

Table 6 also contains the integrated results (from Table 2). Both the sequential and integrated optimized designs have the same pretwist. The integrated approach design has the point of taper initiation further outboard and a larger taper ratio than the sequential approach design. Both designs have the largest tuning mass at about the same location (0.40R). The integrated design has larger tuning masses and thus weighs more but has a better autorotational inertia capability than the sequential design. Both designs reduce power required in hover by the same amount. The integrated design requires slightly less forward flight power, but more maneuver power. Both designs have acceptable frequencies. The integrated design has frequencies in the same windows as the initial design. The sequential design has two frequencies which have shifted windows (f_6 and t_2). The largest difference between the two designs is in the hub shear values. The sequential design increases both forward flight and maneuver hub shears by 14.2 and 38.9 percent over the initial design values, respectively. The integrated design reduces forward flight hub shear by 13.7 percent and maneuver hub shear by 3.2 percent over the initial design.

The blade stiffnesses are presented in Fig. 7 for the initial, sequentially-optimized, and integrated-optimized designs. For the sequentially-optimized design, the chordwise bending stiffness EI_{xx} is higher inboard of 0.5R than the initial design and less stiff outboard (see Fig. 7a). The integrated design EI_{xx} is higher than the sequential design to 0.45R. The sequential design flapwise bending stiffness EI_{zz} is slightly higher inboard of 0.30 R and less outboard than the initial design, while the integrated design has an EI_{zz} distribution higher than the initial distribution until around 0.55R (see Fig. 7b). Relative to the initial design, the torsional stiffness GJ for the sequentially-optimized design inboard of the point of taper initiation is the same, while outboard the stiffness has decreased (see Fig. 7c). For the integrated design the GJ distribution is higher than that of the sequential design.

Case 2 Objective Function - To see if the advantage of the integrated approach is dependent on the choice of objective function, the integrated and sequential approaches are compared for the case where only hover performance and dynamics are included in the objective function. In Step 1, the objective function in Eqn.11 becomes

$$F = \frac{P_h}{P_{h_{ref}}} \tag{14}$$

where $P_{h_{ref}}$ is 15 hp. The performance-optimized design shown in the column labelled "Performance" of Table 7 changed the pretwist from -9.0 to -16.0 degrees, the planform from rectangular to tapered with the point of taper initiation at 0.63R, a taper ratio of 1.28, and a root chord of 4.04 in. This design required 14.4 hp, 12.6 hp, and 11.9 hp in hover, forward flight, and maneuver, respectively. As before in the performance optimization step in Case 1, there is a shift in blade frequencies resulting in two frequencies being too close to a per rev value (f_6=8.99 per rev which is too close to 9 per rev and t_2=14.94 per rev which is too close to 15 per rev). As before the autorotational inertia is inadequate since the initial blade has inadequate autorotational inertia.

In the dynamic optimization of Step 2, the objective function in Eqn. 11 becomes

$$F = \frac{S_{4_{ff}}}{S_{4_{ref}}} \tag{15}$$

where $S_{4_{ref}}$ is 2 lbf. These results are presented in the column labelled "Dynamics" of Table 7. This final sequentially-optimized design has satisfactory frequencies. Tuning masses are placed between 0.29R and 0.41R. Recall in Case 1 the tuning masses are more localized. The blade weight increases by 3.9 percent from the initial design. The autorotational inertia is acceptable.

Integrated optimum results (from Table 4) are included in Table 7 in the column labelled "Integrated" for comparison. In this case, there is more of a difference between the sequential and integrated designs than in Case 1. The sequential design has more twist, a point of taper initiation more inboard, less taper, and a smaller root chord than the integrated design. The emphasis on the 4 per rev forward flight hub shear in the integrated objective function results in less twist and taper. Using the sequential approach, the forward flight hub shear is reduced by 20.1 percent over the initial design (from 2.19 to 1.75 lbf). The integrated approach gives a design with slightly worse performance than the sequential design but has reduced the 4 per rev hub shear in forward flight 67.6 percent over the initial blade compared with a 20.1 percent reduction for the sequential approach design. Both designs increased the maneuver hub shear significantly.

As shown in Fig. 8a, the sequential approach chordwise bending stiffness EI_{xx} is larger than the initial design stiffness inboard of 0.45R and outboard of 0.82R. The integrated approach design chordwise bending stiffness EI_{xx} is slightly larger than the initial design stiffness inboard of 0.9R. In the sequential approach, the flapwise stiffness EI_{zz} is smaller than the initial blade stiffness, while in the integrated approach the opposite is true (see Fig. 8b). In the sequential approach, the torsional stiffness GJ is the same up to the point of taper initiation and then decreases to the tip compared to the initial GJ, while in the integrated approach the GJ is higher except at the tip (see Fig. 8c).

Concluding Remarks

A fully integrated aerodynamic/dynamic optimization procedure has been developed for helicopter rotor blades. The procedure combines performance and dynamics analyses for hover, forward flight, and maneuver with a general purpose optimizer. The procedure minimizes an objective function which is a composite measure of performance and dynamics. Specifically, the objective function is a linear combination of power required (for hover, forward flight, and maneuver) and vibratory hub shear. The design variables include pretwist, taper initiation, taper ratio, and root chord as well as stiffnesses, tuning masses, and tuning mass locations. Aerodynamics and dynamics constraints are enforced. Aerodynamic constraints consist of limits on power required (in hover, forward flight and maneuver), on stall, trim, and drag divergence Mach number. Dynamic constraints are on frequencies, minimum autorotational inertia, and maximum blade weight.

The procedure is demonstrated for the design of a scale model of a rotor blade for a utility helicopter. Results are presented for two cases. Case 1 has an objective function involving performance (in hover, forward flight, and maneuver) and forward flight dynamics. Case 2 has an objective function involving performance in hover and forward flight dynamics. In the first case, the procedure is able to obtain a design which meets all the design requirements while reducing the power required in hover and forward flight by 7 percent and in maneuver by 4 percent. The 4 per rev vertical hub shear in forward flight is reduced by 14 percent. This design compares favorably with predicted performance of the reference blade for the given flight conditions. In the second case, the optimized design improves the power required in hover and forward flight by 4 percent with no change in the power required in maneuver. However, there is a substantial reduction (68 percent compared to the initial blade) in forward flight hub shear at a cost of a 65 percent increase in maneuver hub shear.

The designs from the integrated procedure are compared with designs from a sequential optimization approach in which the blade is first designed for performance and then optimized for dynamics. Using the Case 1 objective function, the integrated approach is superior to the sequential approach from the standpoint of achieving a better design for both performance and dynamics behavior. Using the Case 2 objective function, the integrated approach design has somewhat worse performance measures. However, the integrated design has significantly lower 4 per rev forward flight vertical hub shear dynamic behavior than the sequential approach design.

References

1. Bennett, R. L.: Application of Optimization Methods to Rotor Design Problems. Vertica, Vol. 7, No. 3, 1983, pp. 201-208.

2. Friedmann, P. P. and Shantakumaran, P.: Optimum Design of Rotor Blades for Vibration Reduction in Forward Flight. Proc. of the 39th Annual Forum of the AHS, May 9-11, 1983, St. Louis, Missouri.

3. Peters, D. A.; Ko, Timothy; Korn, Alfred; and Rossow, Mark P.: Design of Helicopter Rotor Blades for Desired Placements of Natural Frequencies. Proc. of the 39th Annual Forum of the AHS. May 9-11, 1983, St. Louis, Missouri..

4. Davis M. W. and Weller, W. H.: Application of Design Optimization Techniques to Rotor Dynamics Problems. Journal of the American Helicopter Society, Vol 33, No. 3, July 1988.

5. Celi, R. and Friedmann, P. P.: Efficient Structural Optimization of Rotor Blades with Straight and Swept Tips. Proc. of the 13th European Rotorcraft Forum, Arles, France, September 1987. Paper No. 3-1.

6. Chattopadhyay, Aditi; Walsh Joanne L.; and Riley, Michael F.: Integrated Aerodynamic Load/Dynamic Optimization of Helicopter Rotor Blades. Journal of Aircraft, Vol. 28, No. 1, January 1991.

7. Nixon, M. W.: Preliminary Structural Design of Composite Main Rotor Blades for Minimum Weight. NASA TP-2730, July 1987.

8. Walsh, J. L.; Bingham, G. J.; and Riley, M. F.: Optimization Methods Applied to the Aerodynamic Design of Helicopter Rotor Blades. Journal of the American Helicopter Society, Vol 32, No. 4, October 1987.

9. Walsh, Joanne L.: Performance Optimization of Helicopter Rotor Blades. NASA TM-104054, April 1991.

10. Adelman, H. M. and Mantay, W. R.: Integrated Multidisciplinary Optimization of Rotorcraft: A Plan of for Development. NASA TM-101617 (AVSCOM TM 89-B-004). May 1989.

11. Adelman, H. M. and Mantay, W. R.: Integrated Multidisciplinary Optimization of Rotorcraft. Journal of Aircraft, Vol. 28, No. 1, January 1991.

12. He, Chengjian and Peters, David A.: Optimization of Rotor Blades for Combined Structural, Dynamic, and Aerodynamic Properties. Proceedings of the Third Air Force/NASA Symposium on Recent Advances in Multidisciplinary Analysis and Optimization. San Francisco, California, September 24-26, 1990.

13. Straub, F. K.; Callahan, C. B.; and Culp, J. D.: Rotor Design Optimization Using a Multidisciplinary Approach. AIAA Paper No. 91-0477, Presented as the 29th Aerospace Sciences Meeting. Reno, Nevada, January 7-10, 1991.

14. Callahan, C. B. and Straub, F. K.: Design Optimization of Rotor blades for Improved Performance and Vibrations. Proceedings of the 47th Annual Forum of the American Helicopter Society. Phoenix, Arizona, May 6-8, 1991.

15. Sobieszczanski-Sobieski, J.; James, B.; and Dovi, A.: Structural Optimization by Multi-level Decomposition. AIAA Journal, Vol.23, November 1983.

16. Gessow, Alfred; and Myers, Garry C., Jr.: Aerodynamics of the Helicopters. Frederick Unger Publishing Company, New York, 1952.

17. Johnson, Wayne: CAMRAD/JA - A Comprehensive Analytical Model of Rotorcraft Aerodynamics and Dynamics - Johnson Aeronautics Version. Volume I: Theory Manual and Volume II: User's Manual. Johnson Aeronautics, 1988.

18. Vanderplaats, G. N.: CONMIN - A Fortran Program for Constrained Function Minimization. User's Manual. NASA TMX-62282. August 1973.

19. Noonan, Kevin. W.: Aerodynamic Characteristics of Two Rotorcraft Airfoils Designed for Application to the Inboard Region of a Main Rotor Blade. NASA TP-3009, AVSCOM TR-90-B-005. July 1990.

20. Bingham, Gene J.; and Noonan, Kevin W.: Two-Dimensional Aerodynamic Characteristics of Three Rotorcraft Airfoils at Mach Numbers From 0.35 to 0.90. NASA TP-2000, AVRADCOM TR-82_B-2. May 1982.

21. Yeager, W. T.; Mantay, W. R.; Wilbur, M. L.; Cramer, R. G., Jr.; and Singleton, J. D.: Wind-Tunnel Evaluation of an Advanced Main-Rotor Blade Design for a Utility-Class Helicopter. NASA TM 89129, 1987.

Table 1. Design variable bounds, parameters, and flight conditions used in optimization examples

	Design variables	
	Lower bound	Upper bound
Twist (deg)	−20.0	−5.0
Taper initiation (r/R)	0.265	0.985
Taper ratio	0.05	5.0
Root chord (in)	2.70	8.10
EI_{xx} at root (lbm-ft^2)	5000.00	20000.00
EI_{xx} at y_{tr} (lbm-ft^2)	5000.00	20000.00
EI_{xx} at tip (lbm-ft^2)	5000.00	20000.00
EI_{zz} at root (lbm-ft^2)	5.00	1000.00
EI_{zz} at y_{tr} (lbm-ft^2)	5.00	1000.00
EI_{zz} at tip (lbm-ft^2)	5.00	1000.00
GJ at root (lbm-ft^2)	5.00	1000.00
GJ at y_{tr} (lbm-ft^2)	5.00	1000.00
GJ at tip (lbm-ft^2)	5.00	1000.00
m_1 (lbm)	0.0	0.50
m_2 (lbm)	0.0	0.50
m_3 (lbm)	0.0	0.50
y_1 (r/R)	0.24	0.985
y_2 (r/R)	0.24	0.985
y_3 (r/R)	0.24	0.985

Parameters	
AI_{min}	3456 lbm-in^2
$c_{d_{all}}$	0.1
$c_{t_{min}}$	1.0 in
Number of blades	4
Number of aerodynamic segments HOVT CAMRAD/JA	 19 18
Number of structural segments	50
Number of design variables	19
Power available	20 hp
Blade radius	56.22 in
Maximum blade mass	3.5 lbm
Δf	0.1 per rev

Flight conditions			
Rotational velocity		639.5 RPM (in Freon density of 0.006 slug/ft^3)	
Hover tip Mach number		0.628	
	Hover	Forward flight	Maneuver
C_L	0.00810	0.00810	0.00985
C_D	–	−0.000811	−0.000596
Advance ratio	–	0.35	0.30

Table 2. Initial versus integrated optimization design - Case 1 objective function

	Initial Design	Final Design	Change (%)*
Twist (deg)	−9.0	−16.0	
Taper initiation (r/R)	–	0.68	
Taper ratio	1.0	1.79	
Root chord (in)	5.4	4.38	
m_1 (lbm)	0.0	0.150	
m_2 (lbm)	0.0	0.126	
m_3 (lbm)	0.0	0.018	
y_1 (r/R	–	0.396	
y_2 (r/R)	–	0.395	
y_3 (r/R)	–	0.475	
Hover (hp)	15.4	14.4	−6.5
Forward flight (hp)	13.5	12.6	−6.7
Maneuver (hp)	12.3	11.8	−4.1
Weight (lbm)	3.05	3.34	+9.5
AI (lbm-in^2)	3411	3561	+4.4
f_3 (per rev)	2.87	2.72	
f_4 (per rev)	5.57	5.28	
f_5 (per rev)	8.57	8.23	
f_6 (per rev)	9.66	9.21	
t_1 (per rev)	17.28	17.10	
t_2 (per rev)	15.14	15.79	
$S_{4_{ff}}$ (lbf)	2.19	1.89	−13.7
S_{4_m} (lbf)	0.95	0.92	−3.2

$$^*\text{Change} = \frac{\text{Final - Initial}}{\text{Initial}} \text{ X } 100$$

Table 3. Comparison of integrated optimum design (Case 1) with reference blade

	Present Method	Reference Design
Twist (deg)	−16.0	−16.0
Taper initiation (r/R)	0.68	0.8
Taper ratio	1.79	3.0
Root chord (in)	4.38	5.40
Hover (hp)	14.4	14.8
Forward flight (hp)	12.6	13.1
Maneuver (hp)	11.8	11.8
Forward flight hub shear (lbf)	1.89	1.52

Table 4. Initial versus integrated optimization design - Case 2 objective function

	Initial Design	Final Design	Change (%)*
Twist (deg)	−9.0	−8.1	
Taper initiation (r/R)	–	0.80	
Taper ratio	1.0	1.36	
Root chord (in)	5.40	4.50	
m_1 (lbm)	0.0	0.113	
m_2 (lbm)	0.0	0.157	
m_3 (lbm)	0.0	0.039	
y_1 (r/R)	–	0.246	
y_2 (r/R)	–	0.294	
y_3 (r/R)	–	0.414	
Hover (hp)	15.4	14.8	−3.9
Forward flight (hp)	13.5	12.9	−4.4
Maneuver (hp)	12.3	12.2	−0.8
Weight (lbm)	3.05	3.36	+10.2
AI (lbm-in^2)	3411	3501	+2.6
f_3 (per rev)	2.87	2.79	
f_4 (per rev)	5.57	5.45	
f_5 (per rev)	8.57	8.28	
f_6 (per rev)	9.66	9.82	
t_1 (per rev)	17.28	17.10	
t_2 (per rev)	15.14	15.90	
$S_{4_{ff}}$ (lbf)	2.19	0.71	−67.6
S_{4_m} (lbf)	0.95	1.57	+65.3

$$^*\text{Change} = \frac{\text{Final - Initial}}{\text{Initial}} \text{ X } 100$$

Table 5. Comparison of integrated and sequential optimization design procedures

	INTEGRATED	SEQUENTIAL APPROACH	
		Step 1 Performance	Step 2 Dynamics
Objective function	Case 1: eqn. 10 Case 2: eqn. 11	Case 1: eqn. 12 Case 2: eqn. 14	Case 1: eqn. 13 Case 2: eqn. 15
Design variables	θ_{tw}, y_{tr}, c_r/c_t, c_r EI_{xx}, EI_{zz}, GJ @ root EI_{xx}, EI_{zz}, GJ @ y_{tr} EI_{xx}, EI_{zz}, GJ @tip m_1, m_2, m_3 y_1, y_2, y_3	θ_{tw}, y_{tr}, c_r/c_t, c_r	EI_{xx}, EI_{zz}, GJ @ root EI_{xx}, EI_{zz}, GJ @ y_{tr} EI_{xx}, EI_{zz}, GJ @tip m_1, m_2, m_3 y_1, y_2, y_3
Constraints	Aerodynamics Dynamics	Aerodynamics	Dynamics

Table 6. Comparison of sequential versus integrated optimization designs using Case 1 objective function

	Initial Design	Final Design			Sequential Change (%)**	Integrated Change (%)*
		SEQUENTIAL Step 1 Performance	APPROACH Step 2 Dynamics	INTEGRATED		
Twist (deg)	-9.0	-16.0	-16.0	-16.0		
Taper initiation (r/R)	-	0.51	0.51	0.68		
Taper ratio	1.0	1.65	1.65	1.79		
Root chord (in)	5.40	4.73	4.73	4.38		
m_1 (lbm)	0.0	0.0	0.001	0.150		
m_2 (lbm)	0.0	0.0	0.0008	0.126		
m_3 (lbm)	0.0	0.0	0.094	0.018		
y_1 (r/R)	-	-	0.301	0.396		
y_2 (r/R)	-	-	0.351	0.395		
y_3 (r/R)	-	-	0.402	0.475		
Hover (hp)	15.4	14.4	14.4	14.4	-6.5	-6.5
Forward flight (hp)	13.5	12.7	12.7	12.6	-5.9	-6.7
Maneuver (hp)	12.3	11.8	11.8	11.8	-4.1	-3.8
Weight (lbm)	3.05	3.05	3.15	3.34	+3.3	+9.5
AI (lbm-in^2)	3411	3411	3460	3561	+1.4	+4.4
f_3 (per rev)	2.87	2.78	2.76	2.72		
f_4 (per rev)	5.57	5.04	5.10	5.28		
f_5 (per rev)	8.57	8.44	8.57	8.23		
f_6 (per rev)	9.66	8.74	8.89	9.21		
t_1 (per rev)	17.28	17.31	17.10	17.10		
t_2 (per rev)	15.14	14.64	14.90	15.79		
$S_{4_{ff}}$ (lbm)	2.19	2.90	2.50	1.89	+14.2 %	-13.7 %
S_{4_m} (lbm)	0.95	1.45	1.32	0.92	+ 38.9 %	-3.2 %

** Sequential Change $= \frac{\text{Sequential Final - Initial}}{\text{Initial}} \times 100$

* Integrated Change $= \frac{\text{Integrated Final - Initial}}{\text{Initial}} \times 100$

Table 7. Comparison of sequential versus integrated optimization designs using Case 2 objective function

	Initial Design	Final Design			Sequential Change (%)**	Integrated Change (%)*
		SEQUENTIAL Step 1 Performance	APPROACH Step 2 Dynamics	INTEGRATED		
Twist (deg)	-9.0	-16.0	-16.0	-8.1		
Taper initiation (r/R)	-	0.63	0.63	0.80		
Taper ratio	1.0	1.28	1.28	1.36		
Root chord (in)	5.40	4.04	4.04	4.50		
m_1 (lbm)	0.0	0.0	0.072	0.113		
m_2 (lbm)	0.0	0.0	0.006	0.157		
m_3 (lbm)	0.0	0.0	0.043	0.039		
y_1 (r/R)	-	-	0.288	0.246		
y_2 (r/R)	-	-	0.353	0.294		
y_3 (r/R)	-	-	0.413	0.414		
Hover (hp)	15.4	14.4	14.4	14.8	-6.5	-3.9
Forward flight (hp)	13.5	12.6	12.6	12.9	-6.7	-4.4
Maneuver (hp)	12.3	11.9	11.9	12.2	-3.3	-0.8
Weight (lbm)	3.05	3.05	3.17	3.36	+3.9	+10.2
AI (lbm-in^2)	3411	3411	3456	3500	+1.3	+2.6
f_3 (per rev)	2.87	2.82	2.77	2.79		
f_4 (per rev)	5.57	5.24	5.14	5.45		
f_5 (per rev)	8.57	8.58	8.45	8.28		
f_6 (per rev)	9.66	8.99	8.90	9.82		
t_1 (per rev)	17.28	17.30	17.10	17.10		
t_2 (per rev)	15.14	14.94	14.90	15.90		
$S_{4_{ff}}$ (lbf)	2.19	1.75	1.75	0.71	-20.1	-67.6
S_{4_m} (lbf)	0.95	1.39	1.44	1.57	+51.6	+65.3

** Sequential Change = $\frac{\text{Sequential Final - Initial}}{\text{Initial}}$ X 100

* Integrated Change = $\frac{\text{Integrated Final - Initial}}{\text{Initial}}$ X 100

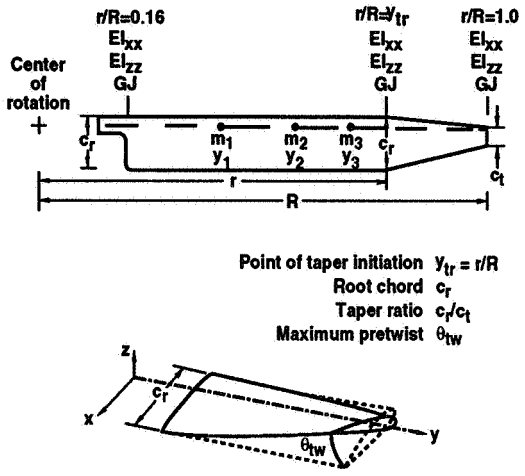

Fig. 1 Rotor blade design variables

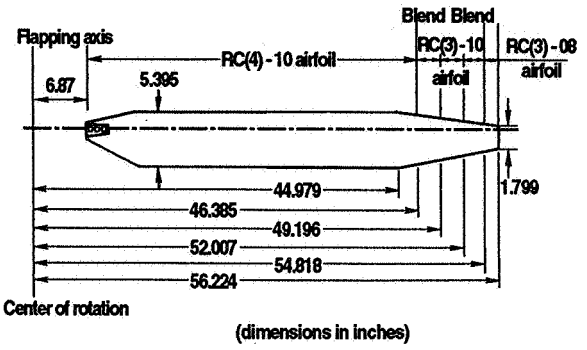

Fig. 3 Reference blade

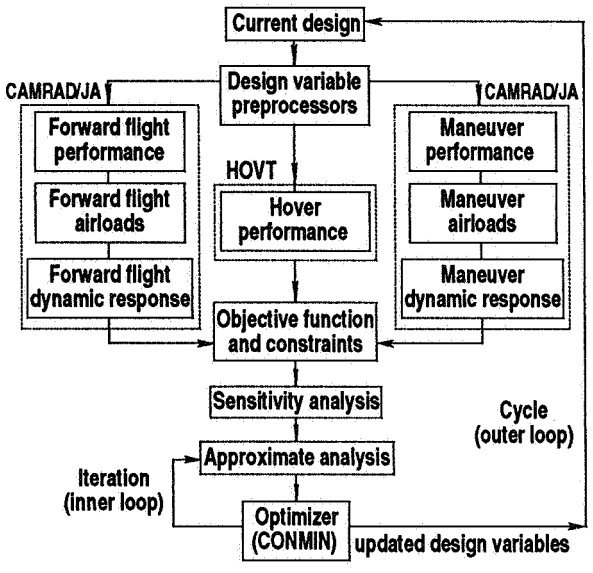

Fig. 2 Optimization procedure

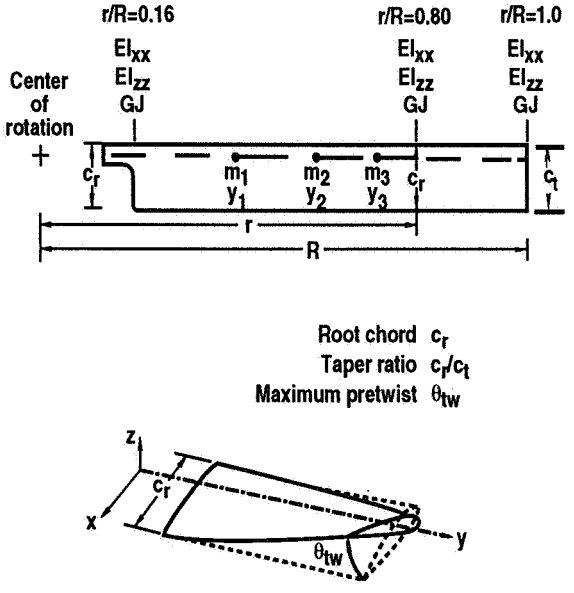

Fig. 4 Initial blade design

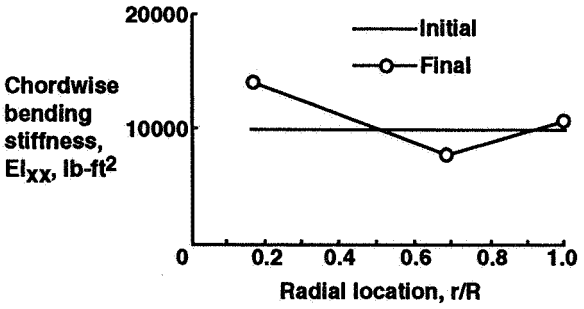

a) Chordwise bending stiffness distribution

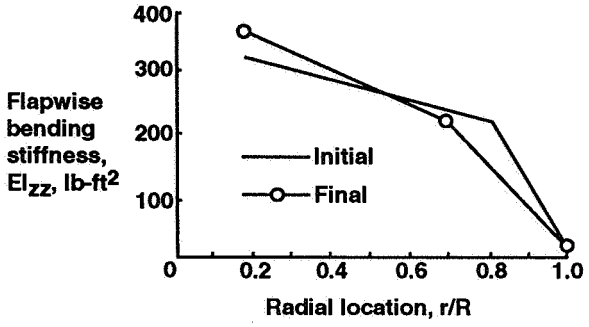

b) Flapwise bending stiffness distribution

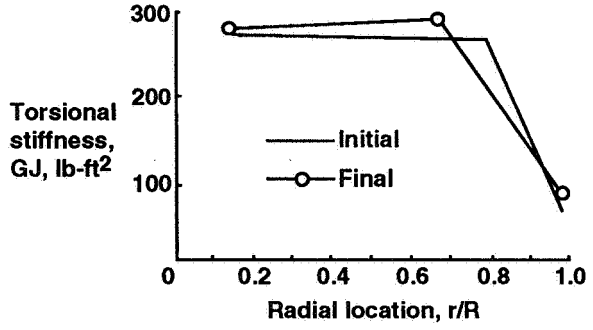

c) Torsional stiffness distribution

Fig. 5 Initial and final stiffness distributions for integrated optimization - Case 1

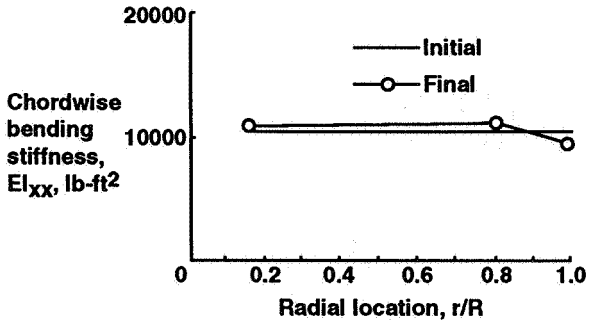

a) Chordwise bending stiffness distribution

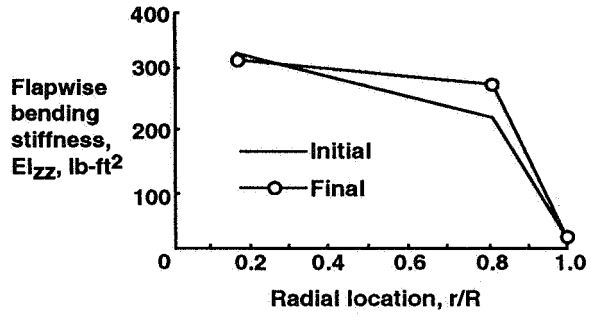

b) Flapwise bending stiffness distribution

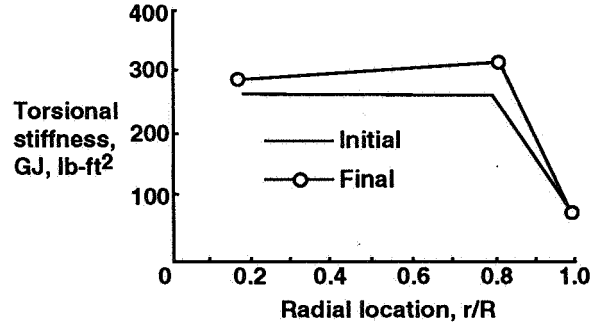

c) Torsional stiffness distribution

Fig. 6 Initial and final stiffness distributions for integrated optimization - Case 2

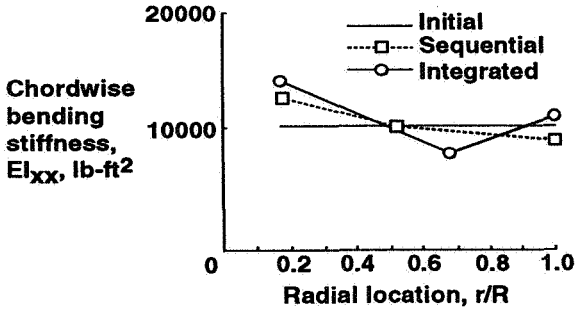

a) Chordwise bending stiffness distribution

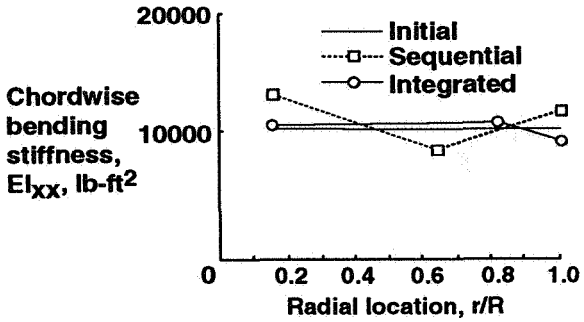

a) Chordwise bending stiffness distribution

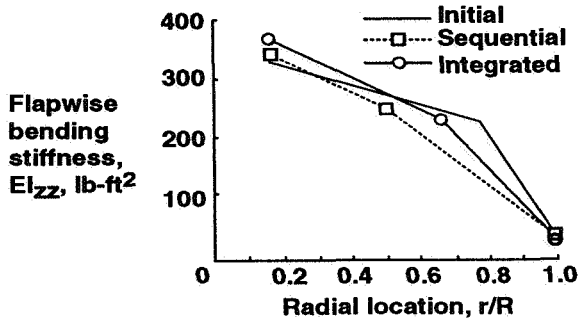

b) Flapwise bending stiffness distribution

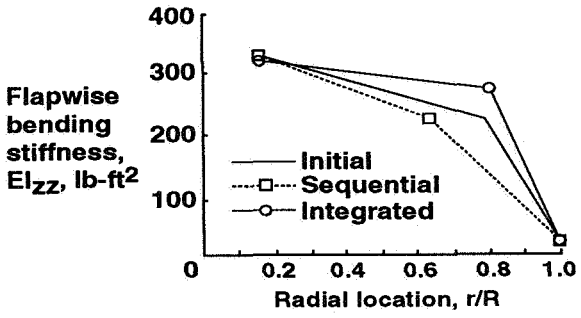

b) Flapwise bending stiffness distribution

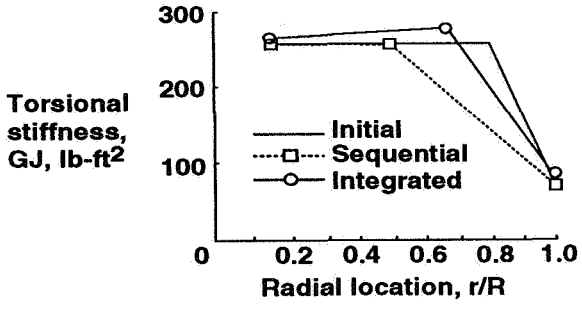

c) Torsional stiffness distribution

Fig. 7) Stiffness distributions for integrated and sequential optimization - Case 1

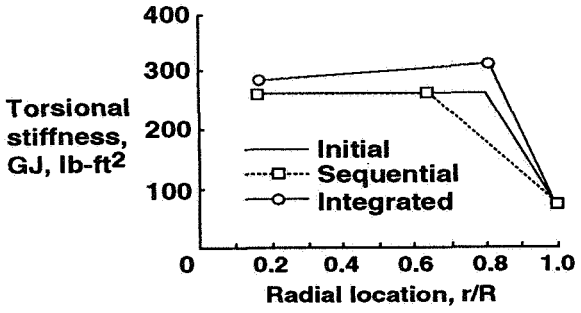

c) Torsional stiffness distribution

Fig. 8 Stiffness distributions for integrated and sequential optimization - Case 2

REPORT DOCUMENTATION PAGE

Form Approved
OMB No. 0704-0188

1. AGENCY USE ONLY *(Leave blank)*	2. REPORT DATE	3. REPORT TYPE AND DATES COVERED
	February 1992	Technical Memorandum

4. TITLE AND SUBTITLE
Fully Integrated Aerodynamic/Dynamic Optimization of Helicopter Rotor Blades

5. FUNDING NUMBERS
505-63-36-06

6. AUTHOR(S)
Joanne L. Walsh
William J. LaMarsh II
Howard M. Adelman

7. PERFORMING ORGANIZATION NAME(S) AND ADDRESS(ES)
NASA Langley Research Center
Hampton, VA 23665-5225

8. PERFORMING ORGANIZATION REPORT NUMBER

9. SPONSORING/MONITORING AGENCY NAME(S) AND ADDRESS(ES)
National Aeronautics and Space Administration
Washington, DC 20546-001

10. SPONSORING/MONITORING AGENCY REPORT NUMBER
NASA TM-104226

11. SUPPLEMENTARY NOTES
Walsh and Adelman: Langley Research Center, Hampton, VA
LaMarsh: UNISYS Corporation, Hampton, VA
Presented at 33rd AIAA/ASME/ASCE/AHS/ASC Structures, Structural Dynamics & Materials Conference, Dallas, Texas, April 13-15, 1992

12a. DISTRIBUTION/AVAILABILITY STATEMENT
Unclassified - Unlimited
Subject Category 05

12b. DISTRIBUTION CODE

13. ABSTRACT *(Maximum 200 words)*
This paper describes a fully integrated aerodynamic/dynamic optimization procedure for helicopter rotor blades. The procedure combines performance and dynamic analyses with a general purpose optimizer. The procedure minimizes a linear combination of power required (in hover, forward flight, and maneuver) and vibratory hub shear. The design variables include pretwist, taper initiation, taper ratio, root chord, blade stiffnesses, tuning masses, and tuning mass locations. Aerodynamic constraints consist of limits on power required in hover, forward flight and maneuver; airfoil section stall; drag divergence Mach number; minimum tip chord; and trim. Dynamic constraints are on frequencies, minimum autorotational inertia, and maximum blade weight. The procedure is demonstrated for two cases. In the first case the objective function involves power required (in hover, forward flight and maneuver) and dynamics. The second case involves only hover power and dynamics. The designs from the integrated procedure are compared with designs from a sequential optimization approach in which the blade is first optimized for performance and then for dynamics. In both cases, the integrated approach is superior.

14. SUBJECT TERMS	15. NUMBER OF PAGES
Helicopter Rotor Blade Optimization Performance, Aerodynamics, Dynamics, CAMRAD/JA, CONMIN	17
	16. PRICE CODE A03

17. SECURITY CLASSIFICATION OF REPORT	18. SECURITY CLASSIFICATION OF THIS PAGE	19. SECURITY CLASSIFICATION OF ABSTRACT	20. LIMITATION OF ABSTRACT
Unclassified	Unclassified	Unclassified	Unlimited